Performance investigation of PEMFC with rectangle blockages in Gas Channel based on field synergy principle

As Published: https://doi.org/10.1007/s00231-018-2473-5

Publisher: Springer Berlin Heidelberg

Persistent URL: https://hdl.handle.net/1721.1/131560

Version: Author's final manuscript: final author's manuscript post peer review, without publisher's formatting or copy editing

Performance Investigation of PEMFC with Rectangle Blockages in Gas Channel Based on Field Synergy Principle

Jun Shen[1], Lingping Zeng[2], Zhichun Liu[1*], Wei Liu

Corresponding Email: zcliu@hust.edu.cn

1.School of Energy and Power Engineering, Huazhong University of Science and Technology, 430074, Wuhan, China

2. Department of Mechanical Engineering, Massachusetts Institute of Technology, Cambridge, Ma 02139-4307, United States

Abstract:

This work, using three-dimension proton exchange membrane fuel cell (PEMFC) model combined with theoretical analysis, is mainly to improve the performance of PEMFC through optimizations of fuel cell structure, adding rectangle blockages in the gas channel. Performance comparison, velocity distribution, interface reactant concentration difference, and pressure drop have been studied in the paper. The result shows that, longitudinal vortices would appear and the performance could be improved with the addition of blockages in the gas channel, especially at high current density with closer arrangement. According to field synergy principle, average mass transfer synergy angle could prove the superiority of optimized structure in the ability of mass transfer. Besides, a novel physical quantity, effective mass transfer coefficient, has been proposed. The effective mass transfer coefficient, is the ability of mass transfer in the direction of electrochemical reaction in PEMFC, which could also give mechanism explanation for the performance improvement.

Key words: PEMFC; rectangle blockages; mass transfer; field synergy

1 Introduction

Due to its high efficiency, low emission, and wide range of application, proton exchange membrane fuel cell (PEMFC), has been considered to be one of the most promising and suitable energy source, instead of traditional fossil fuel. At present, PEMFC is widely and successfully used in many fields such as automobile, communication, submarine and so on. During the process of operation, there is an obvious voltage drop compared with the ideal output voltage, which should be diminished as much as possible. The irreversibility of the fuel cell electrochemical reaction is the main reason of voltage drop, which contains activated overpotential, ohmic overpotential and concentration overpotential. Activated overpotential and ohmic overpotential are related to physical property and the initial operating condition, while the concentration overpotential is determined by the structure and the reaction process of fuel cell. Numerous studies have shown that the mass transfer enhancement is one of the most effective approaches to improve the performance of the PEMFC, but it also is very difficult to conduct. There are three forms of transfer, gases transfer, liquid water transfer and ion transfer during PEMFC operation, and regardless which transfer process, it will directly affect the performance of the fuel cell. Excellent characteristic of mass transfer would supply enough reaction gases to the catalyst layer (CL), accumulate liquid water generated during chemical reaction and remove excess water immediately, and deliver large amounts of proton and electron. Once the mass transfer is hindered, the performance of PEMFC would decrease rapidly. What's more,

undesirable mass transfer process will lead to reaction area uneven distribution, non-uniform temperature distribution, water block and so on, all of which are possible to damage the fuel cell system. So enhancing the process of mass transfer is very important for long-time, high efficiency, and steady operation of PEMFC. Optimizing the structure, and enhancing the mass transfer process of the fuel cell, is a promising approach to improve the performance.

Previous experimental [1-2] and simulation studies have highlighted the influence of the gas diffusion layer on the PEMFC performances. Gerteisen et al. [3] proposed a new customized gas diffusion layer (GDL) design modified by laser-perforation to enhance the liquid water transport from the electrode to the gas channel. It's found that the dynamic and overall performance of the test cell with the perforated GDL were improved, compared with a non-modified GDL. Chun [4] investigated the influence of GDL properties on performance in a PEMFC using one-dimension mixture-phase model. From the numerical simulation, it was found that the PEMFC with GDL having high contact angle, high gas permeability, and thin thickness, performed well, especially at high current density condition. As a result, the best performance is obtained by GDL consists of 200μm thick non-woven carbon paper as gas diffusion medium (GDM) and micro porous layer (MPL) contained 20 wt.% polytetrafluoroethylene (PTFE) content. Sun and co-workers [5] developed a two-dimension cross-the-channel model to study the influence of GDL property and flow-field geometry in the PEMFC cathode catalyst layer. Their results showed that both the electronic conductivity and GDL thickness could be key parameters to influence the transport of reaction gases and the performance. In addition, moderate

GDL compression didn't significantly influence cathode performance for single-phase flow conditions. In order to facilitate the mass transport in gas transport in gas diffusion layer of PEMFC, Chen et al. [6] optimized the GDL using a micro-porous layer fabricated by dry layer preparation, and compared the structure with the conventional wet layer preparation in both physical and electrochemical methods. The PEFMC using dry layer MPLs showed better performance under conditions of high oxygen utilization rate and high humidification temperature of air, so as the mass transport properties of the GDLs. Park et al. [7] focused on the durability and degradation characteristics of GDL in PEMFCs. Mechanical degradation, including compression force effect, freeze/thaw cycle effect, dissolution effect, and erosion effect, and chemical degradation, consisting of the carbon corrosion effect, were the two categorized degradation mechanisms. The degraded GDLs resulted in degradation of fuel cell performance due to lower water management and mass transport.

Besides lots of literature focusing on the GDL property, there were also attentions to be paid to the electrode, flow channel or other parts of the fuel cell. Deshmukh et al. [8] used soft lithography to micropattern the electrodes on the PEMFC in order to enhance the water management and the adequacy of reactant distribution. Compared with a flat electrode, the micropatterned membrane electrode assembly (MEA) showed an increase of power density at higher temperature as well as at higher relative humidity. The approach offered a strategy to eliminate the current use of bipolar plates to stack the MEAs and let the PEMFC systems simple to design and fabricate. The experimental study on the proton exchange membrane (PEM) electrolyzer was carried out by HiroshiIto et al. [9], which focused on the effect of pore

structural properties of current collectors, such as porosity and pore diameter. Results were that when the mean pore diameter of the current collector using titanium (Ti)-felt substrates was larger than 10 μm, the electrolysis performance improved with the decrease of pore diameter. Jhong et al. [10] employed ex-situ X-ray micro-computed tomography (Micro CT) to visualize the catalyst layer structure of three preparation methods. The results indicated that more uniform catalyst distribution and less particle agglomeration, led to better performance. Furthermore, air-brushing catalyst layers showed considerable improvement in fuel cell performance and a significant reduction in electrode-to-electrode variability. Monsaf et al. [11] investigated the effects of the channel width, the number of turns and the flow direction of the spiral channel on the reactants consumption in a PEMFC using a FORTRAN program. The result showed that wider channel, larger number of turns, and the injection of the reactants from the outer side of the spiral channel would enhance the cell performances. Kuo et al.[12-14] adopted a three-dimensional model to investigate the performance characteristics of PEMFC with straight and wave-like gas flow field channel. The results indicated that wave-like channel could enhance the transport of the reaction gases through gas diffusion layer, improve the uniformity of temperature distribution, therefor, the output voltage of the fuel cell had been significantly increased. Bilgili[15] investigated performance of PEMFCs containing obstacles in the anode and cathode gas flow channels. Conducting simulations at different operation conditions, the result showed that the electrochemical reaction was improved and higher cell voltage is obtained at high current densities. Liu et al. [16] combined the optimizations of operating condition and channel structure of PEMFC using multi-objective genetic algorithm. A type of

tapered channel was obtained for providing a higher pressure to enhance the mass transfer of fuel cell, which could improve the output performance. Heidary et al. [17, 18] investigated the effect of in-line and staggered blockage in a parallel flow channels of PEMFC by both numerical modelling and experimental investigation. Results showed that the staggered blockages improved the performance, being better than the baseline case, and the in-line case.

All of the above researches are based on the improved structure, which are little about the mechanism and theory of mass transfer enhancement. Chen [19] et al. developed a convective mass transfer field synergy equation with a specific boundary condition for photocatalytic oxidation reactors. The solution of the field synergy equation gave the optimal flow field in the plate type reactor, which could effectively enhance the laminar mass transfer. The results showed the contaminant removal effectiveness for the discrete double-inclined ribs plate reactor was better than the smooth plate reactor. Cheng [20] presented a novel concept of equivalent internal productivity, which was varied by adjusting the angle between two main variables, velocity field and density gradient field, instead of increasing the energy consumption. The numerical simulation was carried out and the results were in accord with previous theory. The synergy method of mass transfer provided possible effective direction in optimization, design and operation of mass transfer devices.

So far, there were many researches focusing on the enhancement of mass transfer, but the study combining field synergy theory analysis and guidance of the optimization design of PEMFC were not so common. The field synergy principle was proposed by Guo et al. [21], showed that the synergy between velocity vector and temperature field in

convective heat transfer could enhance the heat transfer. Chen et al. [19] extended the field synergy principle to the mass transfer process, and believed that the synergy between velocity vector and concentration gradient could enhance the convective mass transfer. Based on the theory of mass transfer enhancement, combined with field synergy principle, the present paper conducted the investigation of the influence of addition of blocks in the gas channel numerically, of what was considered to mean to improve the performance of fuel cell, and the effects were discussed behind.

2Theoretical Analysis

2.1The mass transfer equation

The equation of two–dimension, steady, constant property mass transfer by diffusion could be written as [20],

$$D(\frac{\partial^2 \rho}{\partial x^2}+\frac{\partial^2 \rho}{\partial y^2})+\dot{n}=0 \tag{1}$$

Where, D、ρ and $\dot{n}$ are diffusion coefficient, density and internal mass generation rate, respectively.

Similarly, the equation of two–dimension, steady, constant property, non-internal generation mass transfer by convection could be written as,

$$u\frac{\partial \rho}{\partial x}+v\frac{\partial \rho}{\partial y}=D(\frac{\partial^2 \rho}{\partial x^2}+\frac{\partial^2 \rho}{\partial y^2}) \tag{2}$$

Because the density varied along the flow direction is far less than the variety along the vertical direction, $\frac{\partial^2 \rho}{\partial x^2}<<\frac{\partial^2 \rho}{\partial y^2}$ and the equation (2) could be simplified,

$$u\frac{\partial \rho}{\partial x}+v\frac{\partial \rho}{\partial y}=D\frac{\partial^2 \rho}{\partial y^2} \tag{3}$$

According to the boundary layer theory, the mass transfer by convection in the concentration boundary layer is equal to the mass transfer by diffusion in the adherent layer, which can be expressed as,

$$\int_0^{\delta}[\vec{V}\cdot\nabla\rho]dy=\cos\theta\int_0^{\delta}[|\vec{V}|\cdot|\nabla\rho|]dy=-D\frac{\partial \rho}{\partial y}\Big|_0^{\delta} \tag{4}$$

Where, θ is the intersection angle of the flow velocity and the density gradient. From the equation above, it could be seen that the ability of mass transfer by convection depend on the flow velocity, the density gradient and the intersection angle of the two vectors. Since the ideal incompressible gas is used in the simulation, the density gradient could be replaced by the concentration gradient. Define a new parameter, effective mass transfer coefficient, which could be expressed as,

$$\beta=\left|v\frac{\partial C}{\partial y}\right| \tag{5}$$

Product of velocity and concentration gradient in a certain direction directly reflects the ability of mass transfer in this direction. In PEMFC, the direction of electrochemical reaction is the effective mass transfer direction.

In addition, the Reynold number would be used in the model assumption. The Reynold number of the reactants could be calculated by the following equation,

$$\mathrm{Re}=\frac{\rho u_g d_e}{\mu} \tag{6}$$

Where, ρ, μ are the density and the dynamic viscosity of the reactants, and

u_g , d_e are the characteristic velocity and the equivalent diameter of the flow field.

2.2 Calculation model

Geometry model

PEMFC is a multi-part device that comprises of collectors, flow channels, gas diffusion layers, catalyst layers and the PEM membrane [22].The structure diagram of PEMFC is shown in the Fig.1 below.

Fig.1 (a) is schematically shown the standard structure of the PEMFC, and the measures for enhancements of mass transfer in our investigation are based on the standard model. And the schematics of PEMFC with adding blockages are shown in the Fig.1 (c) and Fig. 1 (d).

Physical parameters and boundary conditions of numerical simulation

Table 1 shows the geometry size of fuel cell components. The fuel cell with the size below is considered to be the standard of comparison for further improving research. Table 2 presents the physical parameters of PEMFC, which include the gas diffusivity, saturation exponent for pore blockage, porosity and so on. Operation conditions are given in Table 3, including operating pressure, temperature, stoichiometry and so on.

Grid independent test

Due to the regular structure, the model could be meshed by structured hexahedral grids. The simulations were conducted by three different grid sizes. The mesh count of Mesh 1, Mesh 2 and Mesh 3 were 110000, 220000 and 550000, respectively. Based on Mesh 1, Mesh 2 and Mesh 3 refined the meshes of gas

diffusion layers, catalyst layers and membrane. Grid independent test was conducted at current density of 1A·cm^{-2}, and the influence of the grid numbers on the computed results was shown in Table 4. At current density of 1A·cm^{-2}, Mesh 1 and Mesh 3 yielded deviations of approximately 0.01% for the output voltage compared to Mesh 2, shown in Table 4. This indicated that the calculation result was independent of the number of grids, while the number was greater than 110000. Considering the calculation time and calculation accuracy, we chose Mesh 2 as the calculation model, and the mesh information was shown in Table 1.

Model assumption

The assumptions used in developing the model are:

1 The fuel cell performed stably;

2 Ideal incompressible gases were applied;

3 The porous media including GDLs, catalyst layers and membrane were considered to be isotropic, and the membrane should strictly separate the reactant gases;

4 Deal with the liquid water existing in small droplets as gas state

5 The fluid flow in the fuel cell was laminar.

2.3 Governing equations

The 3D model is developed by using ANSYS FLUENT 16.0, a CFD software with a built-in a Fuel Cell and Electrolysis Module based on the finite volume method, including mass, momentum, energy, charge conservation equations and so on. Pressure-Based solver is used to solve non-linear governing equations, and Pressure-Velocity Coupling is done using SIMPLE algorithm during the iteration

process.

Mass conservation equation

$$\frac{\partial(\varepsilon\rho)}{\partial t}+\nabla(\varepsilon\rho\vec{u})=S_m \tag{7}$$

Where, ε is the porosity and S_m is source term of mass conservation, which are solved respectively in different regions.

Momentum conservation equation

$$\frac{\partial(\varepsilon\rho\vec{u})}{\partial t}+\nabla(\varepsilon\rho\vec{u}\vec{u})=-\varepsilon\nabla p+\nabla(\varepsilon\mu\nabla\vec{u})+S_u \tag{8}$$

Where, p, μ, S_u are the pressure, the viscosity, and the momentum source items, respectively. The momentum source terms are different for different regions of the fuel cell. Gravity force, Darcy drag force, surface tension force and electrokinetic force are considered.

Energy conservation equation

$$\frac{\partial(\varepsilon\rho c_p T)}{\partial t}+\nabla(\varepsilon\rho c_p\vec{u}T)=\nabla\cdot(k^{eff}\nabla T)+S_Q \tag{9}$$

c_p represents specific heat capacity at constant pressure, and k^{eff} is the effective thermal conductivity. The energy source term S_Q considers the heat released by the electrochemical reaction, heat due to phase change, ohm heat and the heat transferred from the energy to maintain the electrode reaction rate.

Species conservation equation

$$\frac{\partial(\varepsilon c_k)}{\partial t}+\nabla(\varepsilon\vec{u}c_k)=\nabla\cdot(D_k^{eff}\nabla c_k)+S_k \tag{10}$$

c_k represents species concentration, and D_k^{eff} is the effective diffusion coefficient. For hydrogen and oxygen, species source terms S_k are the mass of reaction. Species source term of liquid water includes the mass of water generation, water transport due to electro-osmotic drag and water condensation due to phase change.

Conservation of charge

$$\nabla(\sigma_s \nabla \phi_s) + R_s = 0 \tag{11}$$

$$\nabla(\sigma_m \nabla \phi_m) + R_m = 0 \tag{12}$$

Where, σ is the electrical conductivity, ϕ is the potential, R_s and R_m are the volumetric transfer currents, subscripts s and m represent solid phase and membrane phase respectively. The source terms representing transfer current could be calculated by using Butler–Volmer equation [23]:

$$R_{an} = R_{an}^{ref} \left(\frac{C_{H_2}}{C_{H_2}^{ref}}\right)^{\gamma_{an}} \left[\exp\left(\frac{\alpha_{an,an} F \eta_{an}}{RT}\right) - \exp\left(-\frac{\alpha_{cat,an} F \eta_{cat}}{RT}\right)\right] \tag{13}$$

$$R_{cat} = R_{cat}^{ref} \left(\frac{C_{O_2}}{C_{O_2}^{ref}}\right)^{\gamma_{cat}} \left[\exp\left(-\frac{\alpha_{cat,cat} F \eta_{cat}}{RT}\right) - \exp\left(\frac{\alpha_{an,cat} F \eta_{cat}}{RT}\right)\right] \tag{14}$$

R_{an}^{ref} and R_{cat}^{ref} are the volumetric reference exchange current density in the anode and in the cathode. F is the Faraday constant, C_i and C_i^{ref} are the species concentration and reference species concentration. η is the activation overpotential, α represents the exchange coefficient and γ stands for the concentration dependence.

The source terms in different conservation equation are shown in the Table 5, and the definition of parameters are shown in the nomenclature.

3 Results and discussion

3.1 Model validation

To evaluate the validity of the present model, the simulation results of the base design was compared with experimental data of Ref. [24] shown in Fig.2. The simulation was operated at 80℃ with fully humidified reactant gases, and backpressure were 3 atm on both the anode and cathode sides. The simulation data showed good agreement with experimental data while the current density was less than 1.2 $A \cdot cm^{-2}$. At higher current density, due to water accumulation and fuel cell attenuation , the experimental performance was poor than that of simulation.

3.2 Simulation results and analysis

In conventional PEMFC, the Reynold number of the reactants are both in the laminar flow range. According to the Eq. (6), the Reynold number of air is 90, while the Reynold number of hydrogen is much less than that of air, due to the smaller velocity and density. The vertical velocity component is so small that the transport of reactant gases from gas channel to the surface of electrode is limited. According to the field synergy principle, set disturbance along the channel will be an effective scheme to increase the vertical velocity component, which enhance the convective mass transfer, and improve the fuel cell performance. Considering the feasibility of processing, rectangle blockage has been chosen. Furthermore, two cases of different

blockage arrangement are set to investigate the influence rules of the blockage density.

Two cases below are compared with the conventional condition:

Standard: conventional straight gas channel

Case 1: blockages equally spaced arranged, and distance of two blockages is 10mm

Case 2: blockages equally spaced arranged, and distance of two blockages is 5mm.

The velocity distribution of three different cross sections at the current density of 2.0 $A \cdot cm^{-2}$, are given in the Fig.3. The distance of the three cross sections from gas inlet are 20mm, 25mm, and 30mm, respectively. The velocity distribution agrees with the pipe flow pattern, that central velocity is much higher than the velocity near the side walls due to the fluid viscosity. No matter in the anode or in the cathode, regular or narrowed cross section of gas channel, the higher velocity areas are all in the center of the channel field. Previous research [25] also has shown that velocity distribution is parabolic and the maximum value deflects to the interface between gas channel and gas diffusion layer. Low velocity near the GDL surface is disadvantageous for gas transfer. And it is obvious to see that the velocity would have a promotion while the blockages are added in the gas channel, especially in the area near the GDL surface. With the increase arrangement density of blockages, the maximum value of velocity reaches to 7.933 $m \cdot s^{-1}$, and the high velocity area takes up more room and disturbance more severe. Even more important, longitudinal vortices could be generated in the flow channel with the addition of blockages, which could

enhance the mass transfer of reactant gases transferring from gas channel to the inside cell. In Case 1, it's found that longitudinal vortices also appear in the area without blockages under the influence of blockages ahead. Moreover, adding blockages in the gas channel will reduce the cross-sectional area and have an increase of the mainstream velocity, which could be conducive to blow the liquid water droplet out of the channel. Periodical change of the cross-sectional area will be well for gas uniform distribution along the direction perpendicular to the direction of flow, so the concentration overpotenial will decrease and the performance of the fuel cell improved.

Fig.4 shows the comparison of polarization curves between different cases. It could be seen that the output voltage would have some rise with addition of rectangle blockages, which is almost 0.02V higher than the fuel cell with conventional straight channel at the current density of 2 $A \cdot cm^{-2}$. At low current density, the output voltage has little improvement, and polarization curves are almost coincided of different cases while the current density is under 1$A \cdot cm^{-2}$. With the increase of current density, the improvement of performance become larger and more evident. Due to constant mass flow setting in the inlet, low current density means a large amount of excess reactant, which would reduce concentration overpotential and promote the performance. In this way, the effect of mass transfer enhanced of blockages addition are reduced in low current density, while presenting advantages in high current density. Moreover, Case 2 shows the best performance in the above figure, indicating that the closer the blockages arranged the better the performance will be.

To make it obvious that performance improvement of different cases is also

given in the Fig.4. Where, V_0 is the output voltage with standard straight gas channel, and ΔV is the voltage difference between the optimized structure and standard structure. The performance improvement grows at a modest pace at low current density, though the improvement isn't obvious. While at high current density, the performance improvement grows sharply, that the curves slope become bigger. With blockages arranged of distance of 5mm, the performance improvement reaches almost 4% at the current density of 2 $A \cdot cm^{-2}$.

The Fig.5 is the relation between current density and average synergy angle theta. According to field synergy theory, the smaller the average synergy angle is, the better ability of the mass transfer would be obtained. As in conjunction with Fig.4, the synergy angle theta of Case 2 should be the smallest, while the theta of standard structure would be the largest. The average angles between velocity vector and concentration gradient in the anode and in the cathode are consistent with the above prediction, that the average synergy angle in the anode decreases from 65^o to 56^o at the current density of 2 $A \cdot cm^{-2}$, and decreases from 55.6^o to 50.6^o in the cathode. In addition, it's found that the change of the synergy angle is larger at low current densities than that at high current densities. This is because more reactants would be consumed and the mass transfer would be enhanced due to the electrochemical reaction, and the enhancement by adding blockages isn't obvious. However, the change tendency are opposite at different current densities in the anode and in the cathode. Since the diffusion coefficient of hydrogen is much larger than the diffusion coefficient of oxygen, the mass transfer enhancement of hydrogen at low current

density is mainly caused by the increase of velocity with a constant inlet mass flow rate. For oxygen, high current density is the cause of the mass transfer enhancement, so the smallest synergy angle appears in the anode at the current density of 0.2 $A \cdot cm^{-2}$, and the smallest angle appears in the cathode at the current density of 2 $A \cdot cm^{-2}$.

The effective mass transfer coefficient varies with the current density in the Fig.6. Whether in the anode or in the cathode, it is found that the novel physical quantity, effective mass transfer coefficient, could exactly reflect the mass transfer ability. In other words, the cell performance is directly related to the effective mass transfer coefficient. Higher effective mass transfer coefficient means high output voltage, which is consistent with the polarization curves of different cases. The best performance case is the Case 2, with blockages arranged of distance of 5mm, the curve of effective mass transfer coefficient of which is over the other two curves. What's more, though in a hydrogen/air PEMFC, the velocity of oxygen in cathode is a few times of the velocity of hydrogen in anode, the anode effective mass transfer coefficient is higher than that in the cathode. This is due to higher diffusion coefficient of hydrogen set at the anode, one order of magnitude higher than that of oxygen set at the cathode, which could be seen in the Table.2.

Fig.7 is the reactant mole concentration of the interface between catalyst layer and gas diffusion layer. With the increase of current density, the mole concentration of reactants decreased gradually, either in the anode or in the cathode. The main reason of the decrease is the larger consumption of reactants, which is proportion to the current density. At the same current density, the case 2 with nearer blockage distance has the higher reactant mole concentration, while the case 1 is lower and the

standard case is the lowest in the three cases. This illustrates that adding blockages in the gas channel could increase the reactant mole concentration of the interfaces in the fuel cell, improve the ability of mass transfer, and the promotion is closely related to the distribution of blockages.

At the same time, Fig.8 shows reactant concentration distribution of the interface between catalyst layer and gas diffusion layer. It's found that reactant concentration reduces linearly in the standard case with straight gas channel. Once the reactant gas flows through a blockage, the concentration of reactant gases will increases. With continuous flowing, the average concentration has a bit promotion. It's why the blockage addition could improve the performance of the fuel cell. Furthermore, the change law would be the same in the interface between catalyst layer and membrane, and the reactant gases concentration of GDL surface determines the amount of reactant gases diffusing into the catalyst layer.

The evolution of pressure drop of cathode with different blockage arrangements is shown in the Fig.9. It's obvious to see that, the closer the blockages arranged, the greater the pressure drop of flow channel is in the cathode. The improvement of fuel cell performance is associated with the increase of the pressure drop at the same time. More parasitic power is needed and the effect of adding blockages should be comprehensively evaluated.

4 Conclusions

Rectangle blockages have been added in the gas channel to improve the performance of PEM fuel cell, and conclusions could be drawn as follows:

(1) Adding blockages in the gas channel, might be regarded as arrangement of

longitudinal vortex generators, is an effective method to enhance the mass transport and the output voltage rise up.

(2) The result shows that the field synergy principle is applicable to structure of gas flow channel with blockages addition for PEM fuel cells, which could give mechanism explanation for the performance improvement.

(3) The addition of the blockages in the flow channel could effectively reduce the angle between the velocity vector and the concentration gradient and enhance the mass transfer of the reactants.

(4) Effective mass transfer coefficient has been proved to be correct, which could exactly reflect the ability of effective mass transfer in the PEM fuel cells.

Acknowledgements

This work is financially supported by the National Natural Science Foundation of China (No. 51376069) and the Key Basic Scientific Research Program (No.2013CB228302).

Nomenclature

c_p	Specific heat capacity	$J \cdot kg^{-1} \cdot k^{-1}$
c_k	Concentration of species i	$kmol \cdot m^{-3}$
c_r	Condensation rate	s^{-1}
c_f	Concentration of sulfonic acid ions	$kmol \cdot m^{-3}$
d_e	Equivalent diameter	m
D	Diffusion coefficient	$m^2 \cdot s^{-1}$
D^{eff}	Effective diffusion coefficient	$m^2 \cdot s^{-1}$
F	Faraday constant 9.6487×10^7	$C \cdot kmol^{-1}$
h_{react}	Net enthalpy change due to the electrochemical reactions	$W \cdot m^{-2} \cdot k^{-1}$
h_L	Enthalpy change due to condensation/vaporization of water	$W \cdot m^{-2} \cdot k^{-1}$
I	Current density	$A \cdot cm^{-2}$
k	Permeability	
k^{eff}	Effective thermal conductivity	$W/(m \cdot K)$
L	Length	m
M_i	Molecular weight of species i	$kg \cdot kmol^{-1}$
n_f	Charge number of sulfonic acid ions	
P	Pressure	$N \cdot m^{-2}$
P_{wv}	Pressure of water vapor	$N \cdot m^{-2}$
P_{sat}	Pressure of saturated water	$N \cdot m^{-2}$

R	Gas constant 8.314	$J \cdot mol^{-1} \cdot k^{-1}$
R_{ohm}	Ohmic resistivity of media	$\Omega \cdot m$
R^{ref}	Reference volumetric transfer current density	$A \cdot m^{-3}$
R_{an}	Anode volumetric transfer current density	$A \cdot m^{-3}$
R_{cat}	Cathode volumetric transfer current density	$A \cdot m^{-3}$
s	Liquid volume fraction	
S	Source term of governing equations	
t	Time	s
T	Temperature	^{o}C
u,v	Velocity components in x, y directions	$m \cdot s^{-1}$

Greek letter

α	Transfer coefficient	
β	Effective mass transfer coefficient	
γ	Concentration dependence	
ε	porosity	
η	Overpotential	V
μ	Dynamic viscosity	$kg \cdot m^{-1} \cdot s^{-1}$
ρ	Density	$kg \cdot m^{-3}$
σ	Electrical conductivity	$\Omega^{-1} \cdot m^{-1}$
ϕ	Electric potential	V

τ_g	Gaseous permeability	m^2
τ_p	Hydraulic permeability	m^2
τ_ϕ	Electrokinetic permeability	m^2
θ	Mass transfer synergy angle	°

References

[1] Passalacqua E, Squadrito G, Lufrano F, et al. Effects of the diffusion layer characteristics on the performance of polymer electrolyte fuel cell electrodes. Journal of Applied Electrochemistry, 2001, 31(4): 449-454.

[2] Ihonen J, Mikkola M, Lindbergh G. Flooding of gas diffusion backing in PEFCs physical and electrochemical characterization. Journal of The Electrochemical Society, 2004, 151(8): A1152-A1161.

[3] Gerteisen D, Heilmann T, Ziegler C. Enhancing liquid water transport by laser perforation of a GDL in a PEM fuel cell. Journal of Power Sources, 2008, 177(1), 348-354

[4] Chun J H, Park K T, Jo D H, et al. Numerical modeling and experimental study of the influence of GDL properties on performance in a PEMFC. International Journal of Hydrogen Energy, 2011, 36(2): 1837-1845.

[5] Sun W, Peppley B A, Karan K. Modeling the influence of GDL and flow-field plate parameters on the reaction distribution in the PEMFC cathode catalyst layer. Journal of Power Sources, 2005, 144(1): 42-53.

[6] Chen J, Xu H, Zhang H, et al. Facilitating mass transport in gas diffusion layer of

PEMFC by fabricating micro-porous layer with dry layer preparation. Journal of Power Sources, 2008, 182(2): 531-539.

[7] Park J, Oh H, Ha T, et al. A review of the gas diffusion layer in proton exchange membrane fuel cells: durability and degradation. Applied Energy, 2015, 155: 866-880.

[8] Deshmukh A B, Kale V S, Dhavale V M, et al. Direct transfer of micro-molded electrodes for enhanced mass transport and water management in PEMFC. Electrochemistry Communications, 2010, 12(11): 1638-1641.

[9] Hiroshi Ito, Tetsuhiko Maeda, et al. Experimental study on porous current collectors of PEM electrolyzers. International Journal of Hydrogen Energy, 2012, 37, 7418–7428.

[10] Jhong H R M, Brushett F R, Kenis P J A. The effects of catalyst layer deposition methodology on electrode performance. Advanced Energy Materials, 2013, 3(5): 589-599.

[11] Monsaf T, Hocine B M, Youcef S, et al. Unsteady three-dimensional numerical study of mass transfer in PEM fuel cell with spiral flow field. International Journal of Hydrogen Energy, 2017, 42(2): 1237-1251.

[12] Kuo J K. Evaluating the enhanced performance of a novel wave-like form gas flow channel in the PEMFC using the field synergy principle. Journal of Power Sources, 2006, 162(2): 1122-1129.

[13] Kuo J K, Yen T H. Three-dimensional numerical analysis of PEM fuel cells with straight and wave-like gas flow fields channels. Journal of Power Sources, 2008, 177(1): 96-103.

[14] Kuo J K, Yen T S. Improvement of performance of gas flow channel in PEM fuel cells. Energy Conversion and Management, 2008, 49(10): 2776-2787.

[15] Bilgili M, Bosomoiu M, Tsotridis G. Gas flow field with obstacles for PEM fuel cells at different operating conditions. International Journal of Hydrogen Energy, 2015, 40(5): 2303-231

[16] Liu Z, Zeng X, Ge Y, et al. Multi-objective optimization of operating conditions and channel structure for a proton exchange membrane fuel cell. International Journal of Heat and Mass Transfer, 2017, 111: 289-298.

[17] Heidary H, Kermani M J, Advani S G, et al. Experimental investigation of in-line and staggered blockages in parallel flowfield channels of PEM fuel cells. International Journal of Hydrogen Energy, 2016, 41(16): 6885-6893.

[18] Heidary H, Kermani M J, Prasad A K, et al. Numerical modelling of in-line and staggered blockages in parallel flowfield channels of PEM fuel cells. International Journal of Hydrogen Energy, 2017, 42(4): 2265-2277.

[19] Chen Q, Meng J. Field synergy analysis and optimization of the convective mass transfer in photocatalytic oxidation reactors. International Journal of Heat and Mass Transfer, 2008, 51(11-12): 2863-2870.

[20] Cheng W L, Han X, Sun H Y. Field synergy action in mass transfer process. Proc. Chin. Soc. Electr. Eng., 2005, 25(13): 105-108. 4

[21] Guo Z Y, Li D Y, Wang B X. A novel concept for convective heat transfer enhancement. International Journal of Heat & Mass Transfer, 1998, 41(14): 2221-2225

[22] Le A D, Zhou B. A generalized numerical model for liquid water in a proton

exchange membrane fuel cell with interdigitated design. Journal of Power Sources, 2009, 193(2): 665-683.

[23] Fluent®6.2 Documentation, Fluent Inc., 2005

[24] Wang L, Husar A, Zhou T, et al. A parametric study of PEM fuel cell performances. International Journal of Hydrogen Energy, 2003, 28(11): 1263-1272

[25] Liu F, Xin M. Simulation of flow and mass transfer characteristics in anode of PEMFC. Journal of Thermal Science and Technology, 2005, 3: 009.

Figure captions

Fig.1 The structure diagram of the PEMFC

(a) Standard structure of the PEMFC

(b) Schematic of PEMFC with addition of blockages

(c) Case 1: L=10 mm

(d) Case 2: L=5 mm

Fig.2 Validation of the simulation data with experimental data

Fig.3 Velocity distribution of PEMFC (i=2.0 $A \cdot cm^{-2}$)

Fig.4 Performance and performance improvement of different cases

Fig.5 Relation between current density and average synergy angle

(a) Relation between current density and anode average synergy angle

(b) Relation between current density and cathode average synergy angle

Fig. 6 Effective mass transfer coefficient of different cases

(a) Anode effective mass transfer coefficient

(b) Cathode effective mass transfer coefficient

Fig.7 Reactant mole concentration of the interface between catalyst layer and gas diffusion layer

(a) H_2 mole concentration; (b) O_2 mole concentration

Fig.8 Distribution of reactant of the interface between catalyst layer and gas diffusion layer

(a) Distribution of H_2 mole concentration

(b) Distribution of O_2 mole concentration

Fig.9 Cathode pressure drop

Fig.1 The structure diagram of the PEMFC

(a) Standard structure of the PEMFC

(b) Schematic of PEMFC with addition of blockages

(c) Case 1: L=10 mm

(d) Case 2: L=5 mm

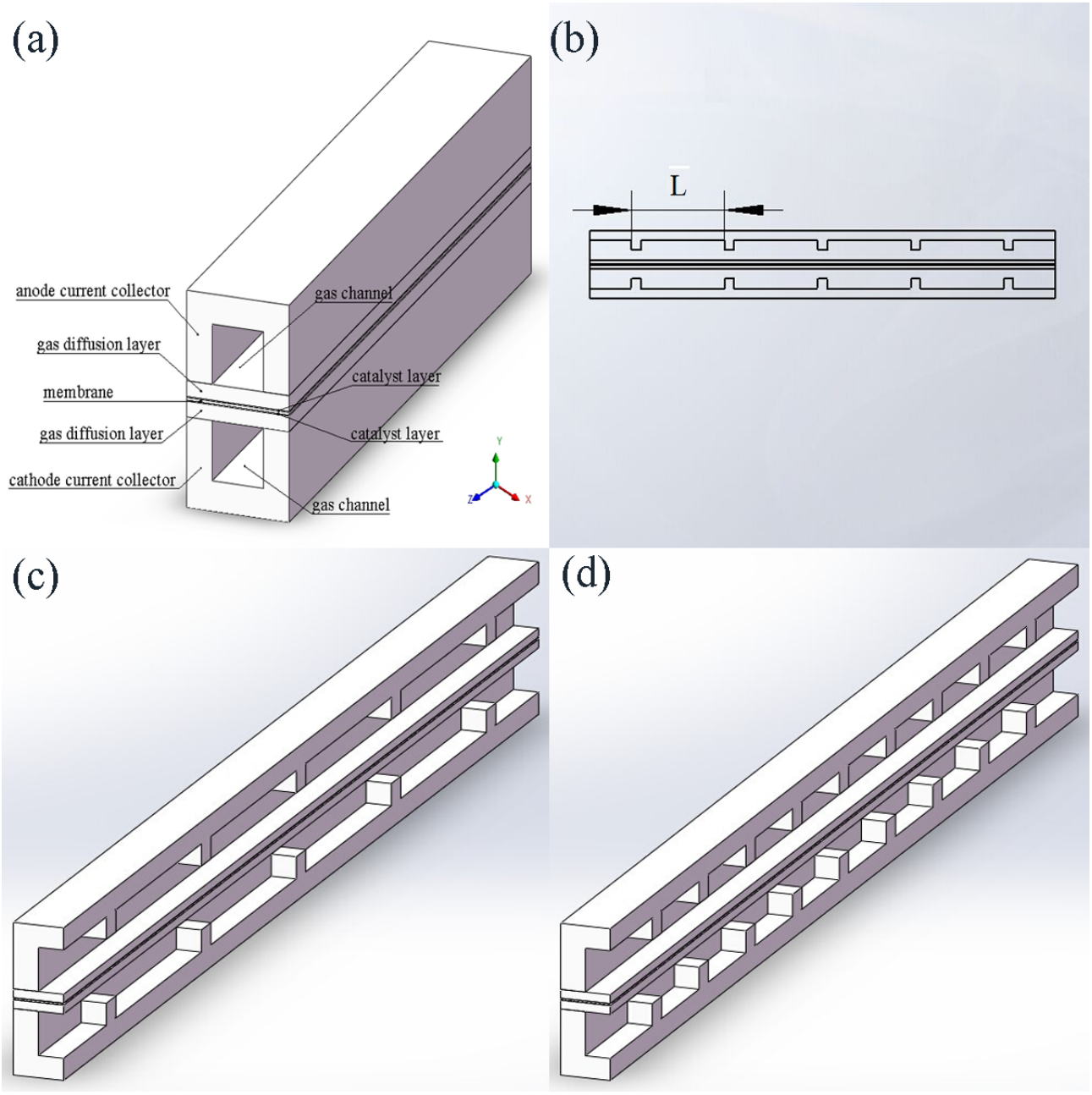

Fig.2 Validation of the simulation data with experimental data

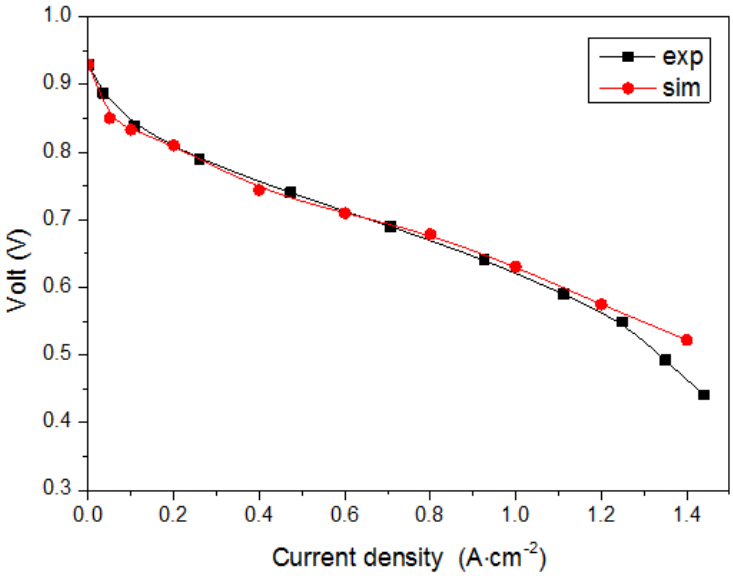

Fig.3 Velocity distribution of PEMFC (i=2.0 A·cm^{-2})

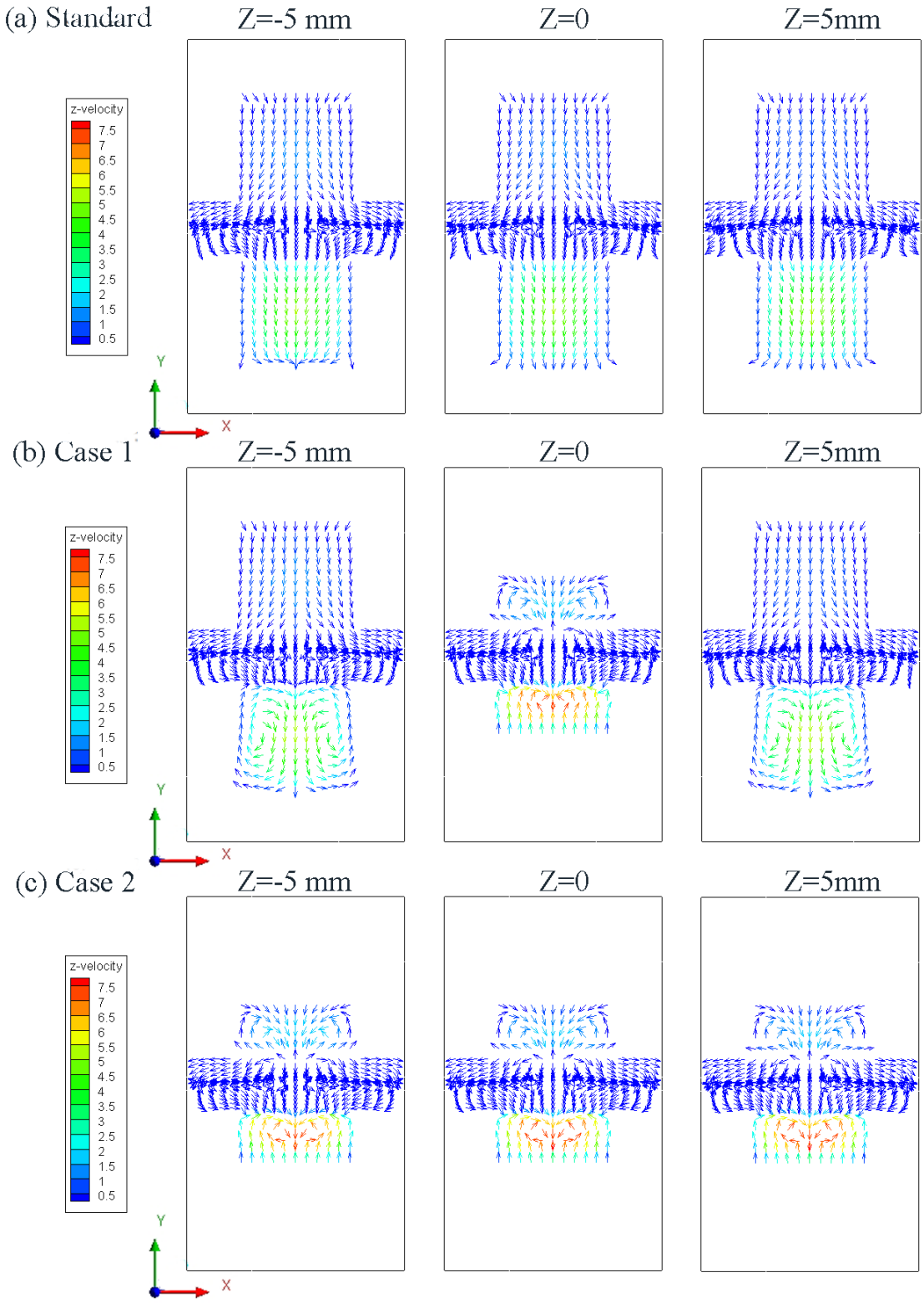

Fig.4 Performance and performance improvement of different cases

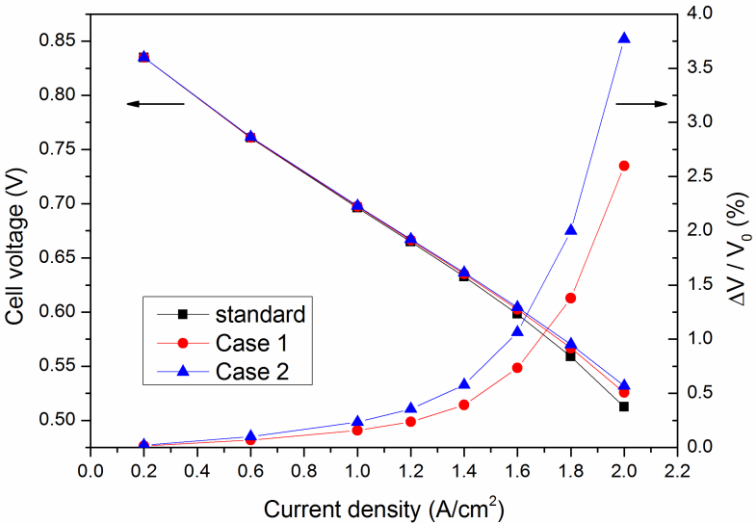

Fig.5 Relation between current density and average synergy angle

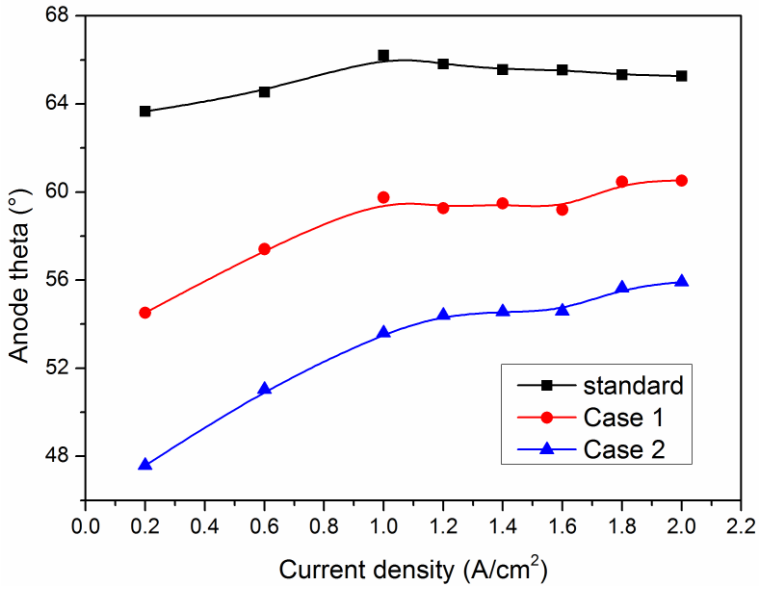

(a) Relation between current density and anode average synergy angle

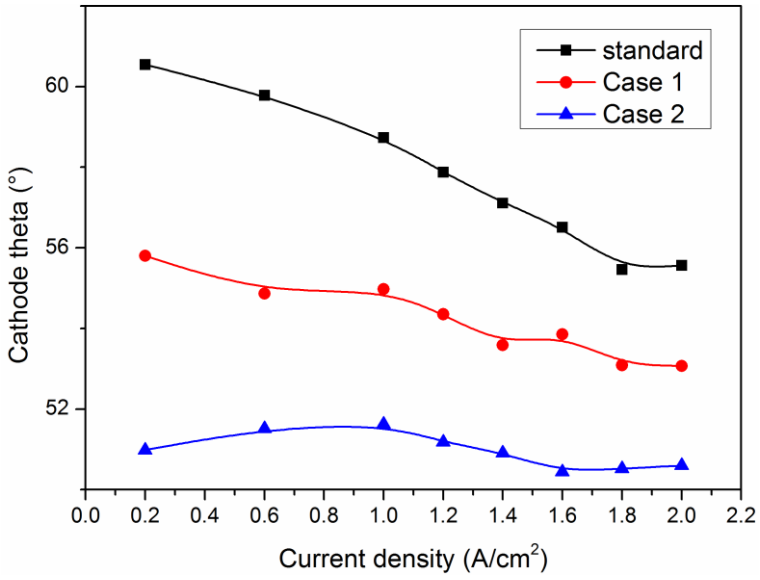

(b) Relation between current density and cathode average synergy angle

Fig. 6 Effective mass transfer coefficient of different cases

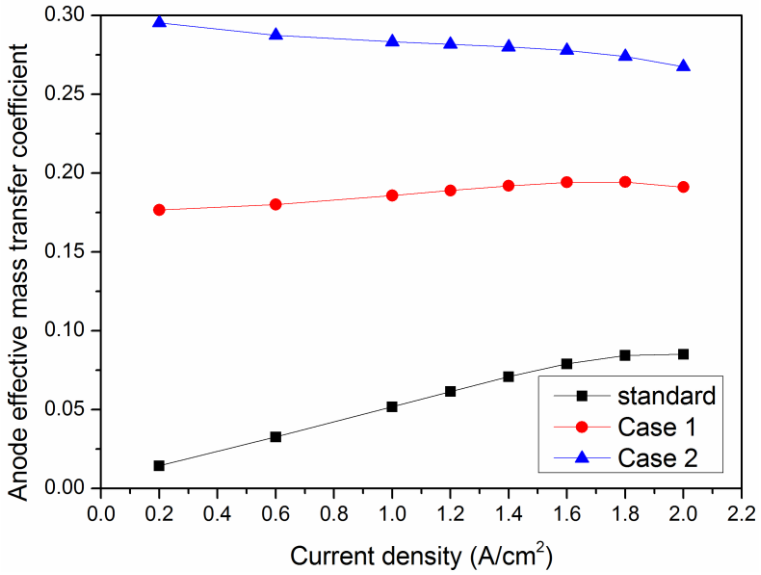

(a) Anode effective mass transfer coefficient

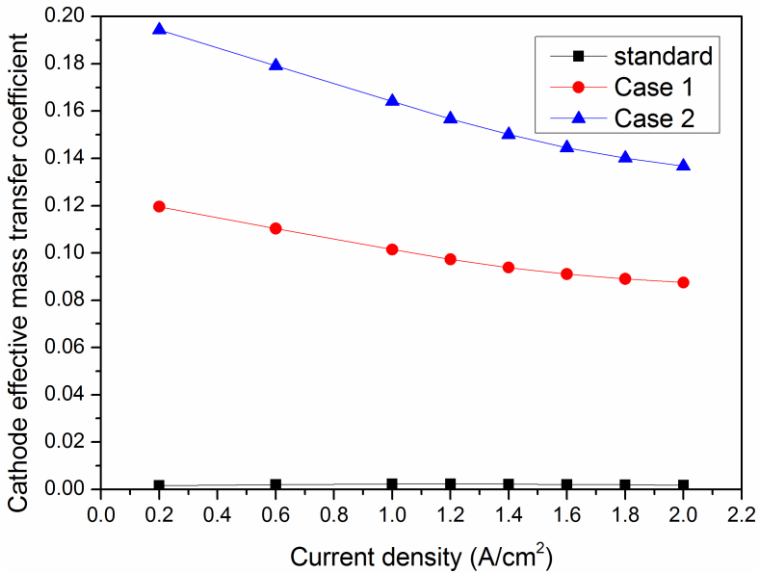

(b) Cathode effective mass transfer coefficient

Fig.7 Reactant mole concentration of the interface between catalyst layer and gas diffusion layer at different current densities

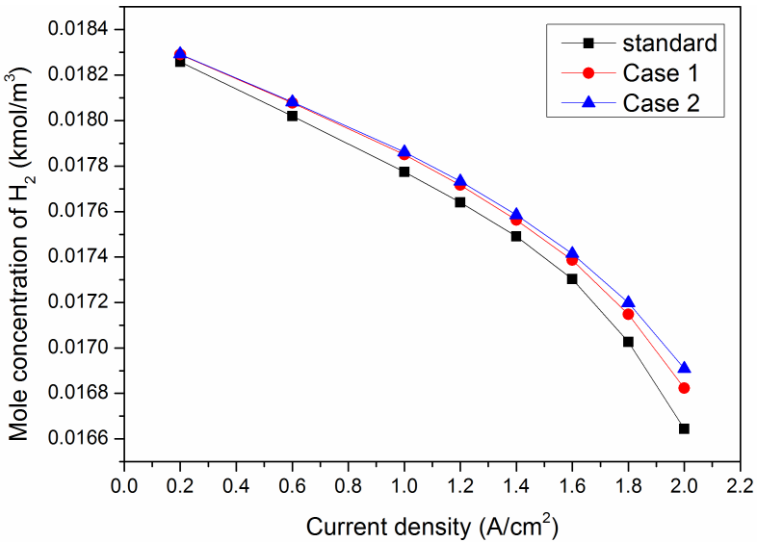

(a) H_2 mole concentration

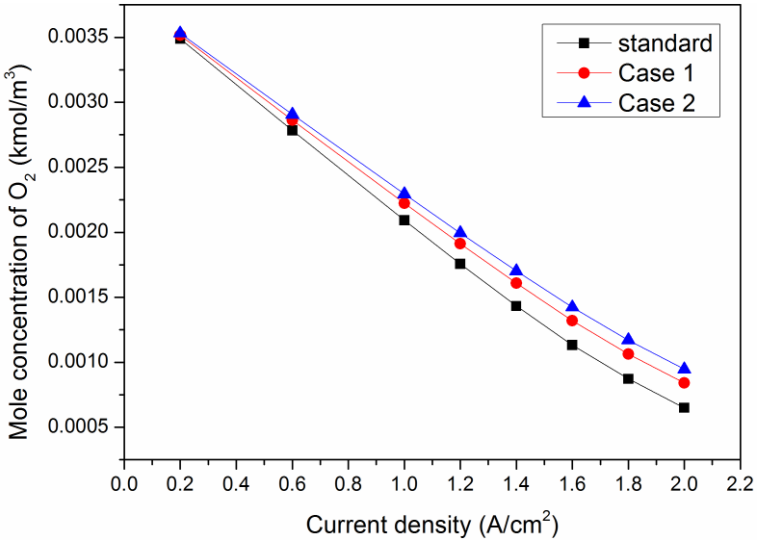

(b) O_2 mole concentration

Fig.8 Distribution of reactant of the interface between catalyst layer and gas diffusion layer

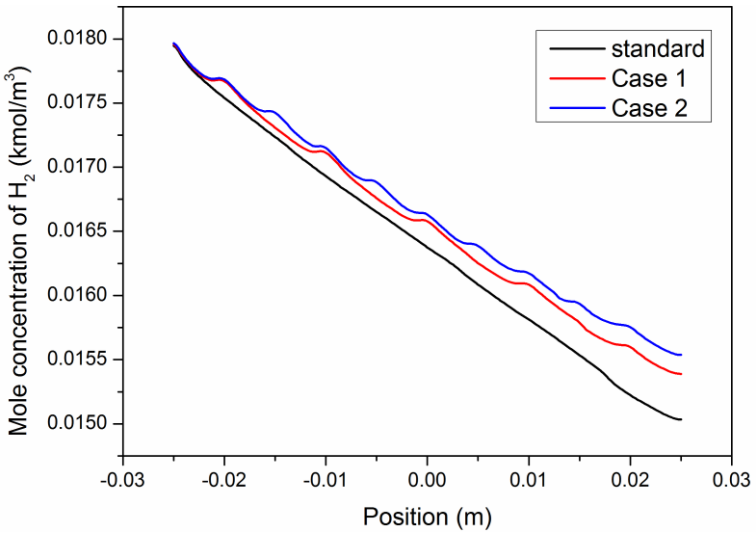

(a) Distribution of H_2 mole concentration

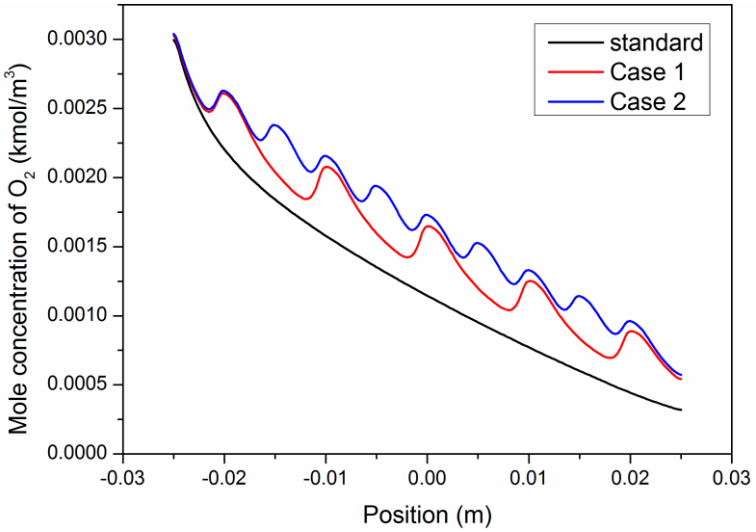

(b) Distribution of O_2 mole concentration

Fig.9 Cathode pressure drop

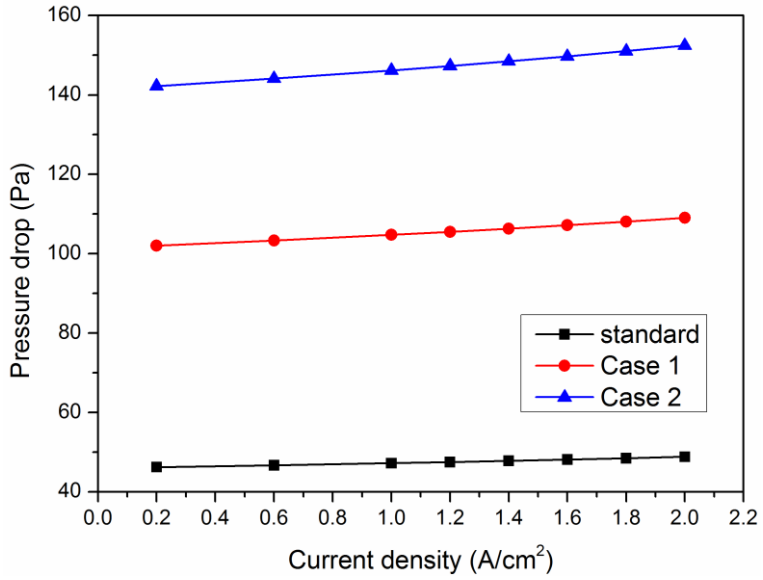

Table 1 Physical dimension and mesh

	Thickness (mm) / Mesh	Width (mm) / Mesh	Depth (mm) / Mesh
Current collector	1.5 / 15	2 / 20	50 / 200
Gas channel	1 / 10	1 / 10	50 / 200
Gas diffusion layer	0.2 / 5	2 / 20	50 / 200
Catalyst layer	0.01 / 5	2 / 20	50 / 200
Membrane	0.025 / 5	2 / 20	50 / 200

Table 2 Physical parameters

Parameters	
Hydrogen diffusivity(m^2/s)	1.1×10^{-4}
Oxygen diffusivity (m^2/s)	3.2×10^{-5}
Water vapor diffusivity (m^2/s)	7.35×10^{-5}
The other species diffusivity (m^2/s)	1.1×10^{-5}
Saturation exponent for pore blockage	2
GDL porosity	0.5
GDL viscous resistance	1×10^{12}
CL porosity	0.5
CL viscous resistance	1×10^{12}
CL surface/ volume ratio	2×10^{5}
Contact resistivity (ohm-m^2)	2×10^{-6}

Table 3 Operation condition

Parameters		Parameters	
Operating pressure（Pa）	101325	Anode stoichiometric	1.5
Backflow pressure（Pa）	0	Cathode stoichiometric	2
Operating temperature（K）	353	Anode H_2 mass fraction	0.112
Anode inlet temperature（K）	353	Cathode O_2/H_2O mass fraction	0.15/ 0.354
Cathode inlet temperature（K）	353	open circuit voltage (V)	1.066

Table 4 Influence of the grid numbers on the computed results

	Grid number	Voltage V	Relative Deviation %
Mesh 1	110000	0.6917	0.01
Mesh 2	220000	0.6918	-
Mesh 3	550000	0.6919	0.01

Table 5 The source terms of governing equations

Conservation equation	**Source terms**
Conservation of mass	For gas channel and GDLs: $S_m = 0$ For anode catalyst: $S_{ma} = -\frac{M_{H2}}{2F} R_{an}$ For cathode catalyst: $S_{mc} = \frac{M_{H_2O}}{2F} R_{cat} - \frac{M_{O_2}}{4F} R_{cat}$
Conservation of momentum	For GDLs and catalyst layers: $S_u = -\frac{\mu}{\tau_g} \varepsilon^2 \vec{u} + \chi\kappa \frac{2\rho \nabla s_l}{(\rho_l + \rho_g)}$ For membrane: $S_u = -\frac{\mu}{\tau_g} \varepsilon^2 \vec{u} + \chi\kappa \frac{2\rho \nabla s_l}{(\rho_l + \rho_g)} + \frac{\tau_\varphi}{\tau_p} c_f n_f F \nabla \varphi_m$
Conservation of energy	$S_Q = h_{react} + R_{an,cat}\eta_{an,cat} + I^2 R_{ohm} + h_L r_w$
Conservation of species	For gas channel and GDLs: $S_k = 0$ For catalyst: $S_{H_2} = -\frac{1}{2F} R_{an}$ $S_{O_2} = -\frac{1}{4F} R_{cat}$ $S_{H_2O} = \frac{1}{2F} R_{cat}$

Conservation of charge	For anode: $R_s = -R_{an}$ $R_m = +R_{an}$ For cathode: $R_s = +R_{cat}$ $R_m = -R_{cat}$
Liquid water transport	$r_w = c_r \max[(1-s)\frac{p_{wv} - p_{sat}}{RT} M_{H_2O} - s\rho_1]$